



Characterization of electro-conductive textile materials by its biaxial anisotropy coefficient and resistivity

Magdalena Tokarska¹

Received: 11 July 2018 / Accepted: 5 January 2019 / Published online: 17 January 2019
© The Author(s) 2019

Abstract

Woven and knitted fabrics were chosen to determine their electro-conductive properties. Van der Pauw equation modified by Wasscher for anisotropic materials was used. The electrical conductivity of textile materials was anisotropic as indicated by the biaxial anisotropy coefficient being in the range from 1.1 to 7.2. Resistance was higher when current flows between electrodes arranged on the line parallel to the warp and course direction in the case of woven or knitted fabrics respectively. Results of analysis confirmed the effect of sample surface roughness on its electro-conductive properties. Sample with a smooth surface will conduct electrical current better than sample with a rough one. Electrical resistivity of the fabrics indicated that they can be used as paths for conveying electrical signals.

1 Introduction

Recently, electro-conductive woven and knitted fabrics have received attention due to their potential applications as electronic components such as transmission lines having the form of conductors connecting individual electronic systems [1], textile antennas being the components to be integrated in electronic systems implemented in smart garments [2], or textile sensors for monitoring human physiological parameters [3, 4]. Most textile-based sensors rely on the change in resistance. The relatively wide range of resistance values is needed for samples intended for textile-based sensor such as strain sensors [3] or temperature sensors [4]. Fixed values at a certain level are required for flat textile products intended for the manufacture of medical electrodes [5], electromagnetic interference shielding textiles [6] or textiles conveying electrical signals [1, 2]. It means that the product is stable in working conditions. Good electrical properties can be obtained applying electro-conductive thin layers by printing [7], magnetron sputtering [8] or electroless plating [9] on surface of an insulative textile substrate. Applications of textile materials depending on their surface resistance are shown in Fig. 1. The insulative textile materials have also

a wide range of applications. They can provide protection against heat and fire or against cold. The materials are used for industrial filtration, geotechnical engineering or sustainable energy protection [10]. However, they are not the subject of interests in the paper.

Electrical conductivity of flat textile materials results from the electrical conductivity of their components i.e. fibers and threads [11–14]. It is obvious that electrical conductivity depends on textile material structure. Generally, electro-conductive woven and knitted fabrics can be compared to metal-dielectric composites [14, 15]. Such structures are composed of interlaced conductive threads and pores filled with dielectric air. There are contact points and contact surface between the interlaced threads. Thus, electrical resistivity of woven or knitted structure is dependent on electrical resistivity of linear components, contact resistance of the components and volume fraction of pores. McLachlan model can be used to predict electrical resistivity of fabrics [14, 15]. Contact resistance between two electro-conductive linear components (for example, threads or textile strips) depends on their surface roughness. Two smooth surfaces will be more adhering to each other. For this reason, a lower contact resistance will be expected. Rough surfaces will make the flow of current on the contact surface difficult. Therefore, assessment of fabric surface roughness is important from the point of view of its electro-conductive properties. Textile strips can be used to design woven pressure sensor matrix [16].

✉ Magdalena Tokarska
magdalena.tokarska@p.lodz.pl

¹ Institute of Architecture of Textiles, Lodz University of Technology, 116 Zeromskiego Street, 90-924 Lodz, Poland

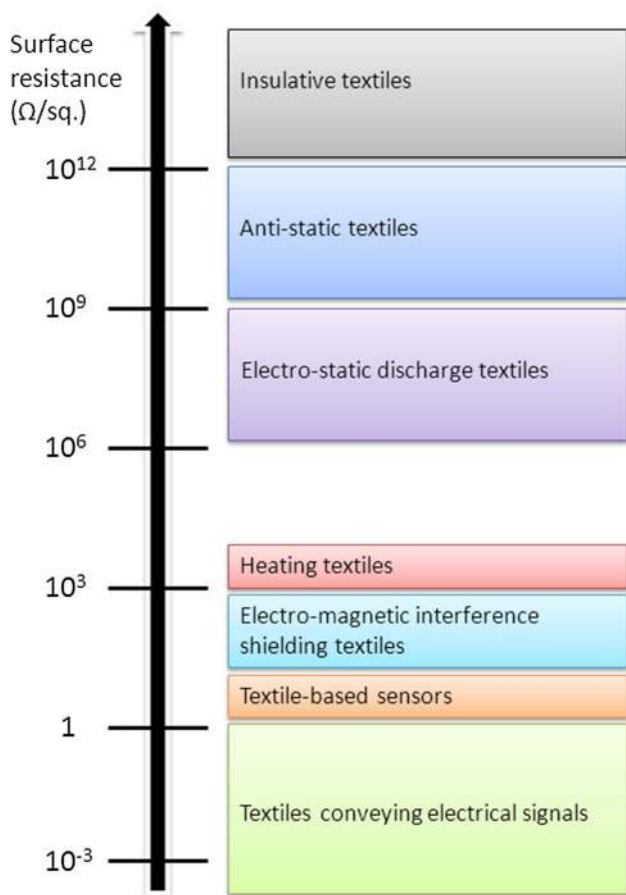


Fig. 1 Possible applications of flat textile materials

Most of textile materials show anisotropic electrical resistance [15, 17, 18]. In order to determine the resistance of this kind of materials and calculate biaxial anisotropy coefficient, most authors apply van der Pauw (vdP) method to solve different problems [15, 17–20]. Van der Pauw [21] developed the method for homogenous isotropic thin uniform and arbitrarily-shaped semiconductor material in order to assess its resistivity. The resistivity ρ of such sample is as follows:

$$\exp\left(-\pi h \frac{R_1}{\rho}\right) + \exp\left(-\pi h \frac{R_2}{\rho}\right) - 1 = 0 \tag{1}$$

where h —the sample thickness; R_1 and R_2 —the resistances in the mutually perpendicular directions of the two-dimensional sample plane.

The vdP Eq. (1) can't be used for textile materials that exhibit anisotropic electrical resistance. Circular and rectangular samples are usually taken into account in studies [22–24]. Wasscher [22] modified the equation for the case of anisotropic samples.

In this paper a new approach to conductivity assessment based on the electrical resistivity determination in combination with analysis of surface roughness of textile material has been shown. Electro-conductive woven and knitted fabrics were taken into consideration due to their different structure. Electro-conductive properties of the fabrics were analyzed based on the vdP equation modified by Wasscher to the case of samples with anisotropic resistivity. The modified equations were used to determine electrical resistivity of circle-shaped woven fabrics and square-shaped knitted fabrics. Analysis of textile sample surface roughness on its electro-conductive properties was presented. It is important from the point of designing woven structure composed of strips cut out from electro-conductive fabrics where contact resistance occurs between textile strips.

2 Materials

In the research electro-conductive woven and knitted fabrics were the subject of interest. The two groups of flat textile products varied in terms of their structure have been selected to show the anisotropy of their electro-conductive properties and the surface roughness. Microscopic images of the fabrics and basic information given by producers are presented in Table 1.

Structural parameters of the textile materials are presented in Tables 2 and 3.

Additionally, parameter D was calculated as a quotient of higher and lower densities and it was used for future analysis.

Next to the estimate of chosen parameter (see Tables 2, 3) the relative expanded uncertainty is given. It was calculated according to the guide [25] and assuming confidence level equal to 0.95.

Table 1 Raw material composition of fabrics

Sample	Description
WF-1	100% polyamide woven fabric; three layers (tin, nickel, silver) metalized
WF-2	100% polyester woven fabric; nickel metalized
WF-3	100% polyester woven fabric; nickel metalized
KF-1	100% polyamide knitted fabric; silver metalized
KF-2	100% polyamide knitted fabric; silver metalized
KF-3	78% polyamide and 22% elastomer knitted fabric; silver metalized

It is assumed that all input quantities x_i needed to determine the output quantity y are independent. Then the combined variance is as follows:

$$u_C^2(y) = \sum_{i=1}^N \left[\left(\frac{\partial f}{\partial x_i} \right)^2 (u_A^2(x_i) + u_B^2(x_i)) \right] \tag{2}$$

where y —the estimate of output quantity; $u_A(x_i)$ —the type A standard uncertainty; $u_B(x_i)$ —the type B standard uncertainty; N —the number of input quantities x_i ($i = 1, 2, \dots, N$); y —the estimate of output quantity; f —the measurement model.

The type A standard uncertainty estimated from n_i independent repeated observations x_i is as follows:

$$u_A(x_i) = \sqrt{\frac{\sum_{k=1}^{n_i} (x_{ik} - \bar{x}_i)^2}{n_i(n_i - 1)}} \tag{3}$$

where \bar{x}_i —the estimate of x_i ; x_{ik} —the k -th observation of x_i .

The type B standard uncertainty is evaluated by scientific judgement based on all of the available information

on the possible variability of input quantity. Assuming a rectangular distribution of possible values, the Type B uncertainty can be determined from the following formula:

$$u_B(x_i) = \frac{d_e}{\sqrt{3}} \tag{4}$$

where d_e —the resolution of measuring instrument.

The expanded uncertainty is expressed as follows:

$$U = k_p u_C(y) \tag{5}$$

where k_p —the coverage factor; for confidence level equal to 0.95, the coverage factor equals 2.

The relative expanded uncertainty was used as a measure of the inaccuracy of the chosen parameters of woven and knitted fabrics given as:

$$U_{rel} = \frac{U}{y} 100\% \tag{6}$$

The uncertainty budgets are presented in Tables 4, 5, 6, 7, 8, 9 and 10.

Table 2 Structural parameters of woven fabrics

Fabric	Thickness	Aerial density	Apparent density	Warp density	Weft density	D
WF-1	0.116 mm (11.2%)	77 g/m ² (2.6%)	666 kg/m ³ (11.1%)	46.0 per 1 cm (1.1%)	41.0 per 1 cm (1.2%)	1.1
WF-2	0.078 mm (15.4%)	75 g/m ² (2.7%)	966 kg/m ³ (15.8%)	40.0 per 1 cm (1.2%)	30.0 per 1 cm (1.7%)	1.3
WF-3	0.270 mm (5.5%)	152 g/m ² (2.6%)	564 kg/m ³ (5.8%)	46.0 per 1 cm (2.2%)	34.0 per 1 cm (1.5%)	1.4

Table 3 Structural parameters of knitted fabrics

Fabric	Thickness	Aerial density	Apparent density	Course density	Wale density	D
KF-1	0.396 mm (4.8%)	139 g/m ² (2.1%)	352 kg/m ³ (5.4%)	52.5 per 1 cm (0.9%)	24.0 per 1 cm (2.1%)	2.2
KF-2	0.388 mm (5.1%)	108 g/m ² (2.8%)	280 kg/m ³ (5.7%)	16.5 per 1 cm (3.0%)	10.0 per 1 cm (5.0%)	1.6
KF-3	0.624 mm (3.0%)	135 g/m ² (2.2%)	216 kg/m ³ (3.7%)	27.0 per 1 cm (1.8%)	26.0 per 1 cm (1.9%)	1.0

Table 4 Uncertainty budget of fabrics thickness determination

Fabric	Estimate of y mm	$u_A^2(x)$ mm ²	$u_B^2(x)^a$ mm ²	$\partial f / \partial x^b$ –	$u_C(y)$ mm	U mm	U_{rel} %
WF-1	0.116	6.0×10^{-6}	3.3×10^{-5}	1	6.3×10^{-3}	0.013	11.2
WF-2	0.078	4.0×10^{-6}	3.3×10^{-5}	1	6.1×10^{-3}	0.012	15.4
WF-3	0.270	2.0×10^{-5}	3.3×10^{-5}	1	7.3×10^{-3}	0.015	5.5
KF-1	0.396	5.6×10^{-5}	3.3×10^{-5}	1	9.4×10^{-3}	0.019	4.8
KF-2	0.388	6.4×10^{-5}	3.3×10^{-5}	1	9.9×10^{-3}	0.020	5.1
KF-3	0.624	5.6×10^{-5}	3.3×10^{-5}	1	9.4×10^{-3}	0.019	3.0

y —the thickness

^aResolution of thickness meter was equal to 0.01 mm

^b $\partial f / \partial x = 1$ because the sample thickness measurement is direct measurement

Table 5 Uncertainty budget of woven fabrics warp density determination

Fabric	Estimate of y Threads per 1 cm	$u_A^2(x)$ (Threads per 1 cm) ²	$u_B^2(x)^a$ (Threads per 1 cm) ²	$\partial f/\partial x^b$ –	$u_C(y)$ Threads per 1 cm	U Threads per 1 cm	U_{rel} %
WF-1	46.0	0.00	0.08	1	0.29	0.5	1.1
WF-2	40.0	0.00	0.08	1	0.29	0.5	1.2
WF-3	46.0	0.11	0.08	1	0.44	1.0	2.2

y—the warp density

^aThe accuracy with which the threads were counted was 0.5 thread

^b $\partial f/\partial x = 1$ because the warp density measurement is direct measurement

Table 6 Uncertainty budget of woven fabrics weft density determination

Fabric	Estimate of y Threads per 1 cm	$u_A^2(x)$ (Threads per 1 cm) ²	$u_B^2(x)^a$ (Threads per 1 cm) ²	$\partial f/\partial x^b$ –	$u_C(y)$ Threads per 1 cm	U Threads per 1 cm	U_{rel} %
WF-1	41.0	0.03	0.08	1	0.34	0.5	1.2
WF-2	30.0	0.01	0.08	1	0.30	0.5	1.7
WF-3	34.0	0.01	0.08	1	0.30	0.5	1.5

y—the weft density

^aThe accuracy with which the threads were counted was 0.5 thread

^b $\partial f/\partial x = 1$ because the weft density measurement is direct measurement

Table 7 Uncertainty budget of knitted fabrics course density determination

Fabric	Estimate of y Courses per 1 cm	$u_A^2(x)$ (Courses per 1 cm) ²	$u_B^2(x)^a$ (Courses per 1 cm) ²	$\partial f/\partial x^b$ –	$u_C(y)$ Courses per 1 cm	U Courses per 1 cm	U_{rel} %
KF-1	52.5	0.03	0.08	1	0.34	0.5	0.9
KF-2	16.5	0.03	0.08	1	0.34	0.5	3.0
KF-3	27.0	0.03	0.08	1	0.34	0.5	1.8

y—the course density

^aThe accuracy with which the courses were counted was 0.5 course

^b $\partial f/\partial x = 1$ because the course density measurement is direct measurement

Table 8 Uncertainty budget of knitted fabrics wale density determination

Fabric	Estimate of y Wales per 1 cm	$u_A^2(x)$ (Wales per 1 cm) ²	$u_B^2(x)^a$ (Wales per 1 cm) ²	$\partial f/\partial x^b$ –	$u_C(y)$ Wales per 1 cm	U Wales per 1 cm	U_{rel} %
KF-1	24.0	0.00	0.08	1	0.29	0.5	2.1
KF-2	10.0	0.03	0.08	1	0.34	0.5	5.0
KF-3	26.0	0.00	0.08	1	0.29	0.5	1.9

y—the wale density

^aThe accuracy with which the wales were counted was 0.5 wale

^b $\partial f/\partial x = 1$ because the wale density measurement is direct measurement

3 Methods

Circle-shaped samples with diameter of 100 mm were prepared from the electro-conductive woven fabrics and square-shaped samples with side of 100 mm were prepared

from the electro-conductive knitted fabrics. In order to determine the surface resistivity of the fabrics vdP method was applied. Four sufficiently small electrodes (A, B, C, D) were arranged at sample in the shape of a square with a side of 60 mm (Fig. 2).

Table 9 Uncertainty budget of fabrics aerial density determination

Fabric	Estimate of y g/m ²	$u^2_A(x_1)$ g ²	$u^2_B(x_1)^a$ g ²	$\partial f/\partial x_1$ 1/m ²	$u^2_B(x_2)^b$ m ²	$\partial f/\partial x_2$ g/m ³	$u_C(y)$ g/m ²	U g/m ²	U_{rel} %
WF-1	77	1.8×10^{-7}	3.3×10^{-9}	127	3.3×10^{-7}	-1544	0.89	2	2.6
WF-2	75	1.2×10^{-6}	3.3×10^{-9}	127	3.3×10^{-7}	-1506	0.88	2	2.7
WF-3	152	1.4×10^{-6}	3.3×10^{-9}	127	3.3×10^{-7}	-3048	1.77	4	2.6
KF-1	139	6.9×10^{-7}	3.3×10^{-9}	100	3.3×10^{-7}	-2789	1.61	3	2.1
KF-2	108	6.2×10^{-7}	3.3×10^{-9}	100	3.3×10^{-7}	-2169	1.25	3	2.8
KF-3	135	1.3×10^{-7}	3.3×10^{-9}	100	3.3×10^{-7}	-2697	1.56	3	2.2

y —the aerial density

x_2 —the diameter of the circular sample or the side length of the square sample; $u^2_A(x_2)=0$ was adopted

x_1 —the mass

^aResolution of weight was equal to 0.0001 g

^bResolution of ruler was equal to 1 mm

Table 10 Uncertainty budget of fabrics apparent density determination

Fabric	Estimate of y kg/m ³	$u^2_A(x_1)$ kg ²	$u^2_B(x_1)^a$ kg ²	$\partial f/\partial x_1$ 1/m ³	$u^2_B(x_2)^b$ m ²	$\partial f/\partial x_2$ kg/m ⁴	$u^2_A(x_3)$ m ²	$u^2_B(x_3)^c$ m ²	$\partial f/\partial x_3$ kg/m ⁴	$u_C(y)$ kg/m ³	U kg/m ³	U_{rel} %
WF-1	666	1.8×10^{-13}	3.3×10^{-15}	1,097,620	3.3×10^{-7}	-13,312	6.0×10^{-12}	3.3×10^{-11}	-5,737,900	0.89	2	2.6
WF-2	966	1.2×10^{-12}	3.3×10^{-15}	1,632,360	3.3×10^{-7}	-19,314	4.0×10^{-12}	3.3×10^{-11}	-12,380,800	0.88	2	2.7
WF-3	564	1.4×10^{-12}	3.3×10^{-15}	471,570	3.3×10^{-7}	-11,289	2.0×10^{-11}	3.3×10^{-11}	-2,090,630	1.77	4	2.6
KF-1	352	6.9×10^{-13}	3.3×10^{-15}	252,525	3.3×10^{-7}	-7020	5.6×10^{-11}	3.3×10^{-11}	-886,389	1.61	3	2.1
KF-2	280	6.2×10^{-13}	3.3×10^{-15}	257,732	3.3×10^{-7}	-5567	6.4×10^{-11}	3.3×10^{-11}	-717,398	1.25	3	2.8
KF-3	216	1.3×10^{-13}	3.3×10^{-15}	160,256	3.3×10^{-7}	-4327	5.6×10^{-11}	3.3×10^{-11}	-346,709	1.56	3	2.2

y —the apparent density

x_2 —the diameter of the circular sample or the side length of the square sample; $u^2_A(x_2)=0$ was adopted

x_1 —the mass

x_3 —the thickness

^aResolution of weight was equal to 0.0001 g

^bResolution of ruler was equal to 1 mm

^cResolution of thickness meter was equal to 0.01 mm

Line connected electrodes A and B (or D and C) was parallel to the warp or course direction (Fig. 2a). Line connected electrodes A and D (or B and C) was parallel to the weft or wale direction (Fig. 2b). The measurement conditions were in accordance with the standard [26]. Resistance R_{11} was obtained when direct current I_{DC} was fed through the electrodes D and C and the voltage drop U_{AB} between electrodes A and B was measured (variant 1). Resistance R_{12} was obtained when direct current I_{AB} was fed through the electrodes A and B and the voltage drop U_{DC} between electrodes D and C was measured (variant 3). Resistance R_{21} was obtained when direct current I_{BC} was fed through the electrodes B and C and the voltage drop U_{AD} between electrodes A and D was measured (variant 2). Resistance R_{22} was obtained when direct current I_{AD} was fed through the electrodes A and D and the voltage drop U_{BC} between electrodes B and C was measured (variant 4).

Based on analysis of sample geometry and electrodes arrangement it was found the distance between single electrode and sample edge. The distances are equal to $d_c = 7.6$ mm and $d_r = 28.3$ mm in case of circle-shaped and square-shaped samples respectively (see Fig. 2). To predict resistances on the sample edges additionally electrodes were arranged in the shape of a square with a side of 40 mm and next with a side of 20 mm. The mean resistances R_1 and R_2 were determined for all electrodes arrangements based on following dependences:

$$R_1 = 0.5(R_{11} + R_{12}) \tag{7}$$

$$R_2 = 0.5(R_{21} + R_{22}) \tag{8}$$

Based on results of measurements and using procedure proposed by Tokarska and Orpel [27] the resistances R_1 and R_2 on sample edges were predicted in order to determine

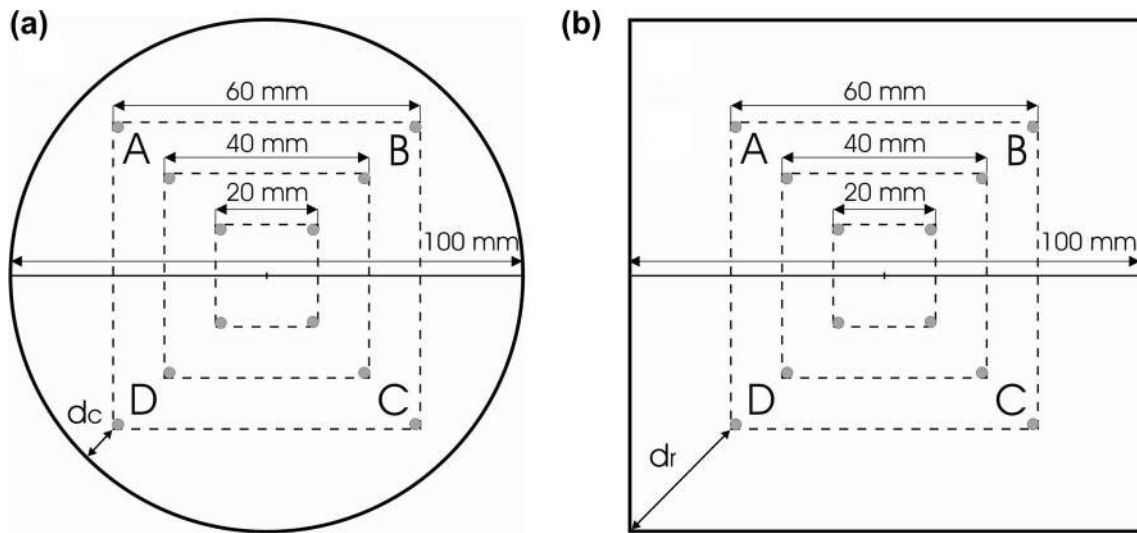


Fig. 2 **a** Electrodes arrangement for a circle-shaped sample, **b** electrodes arrangement for a square-shaped sample

the resistivity ρ and surface resistance R_s for the electro-conductive fabrics.

Based on Wasscher’s extension of the method of vdP to the case of circular sample the resistivity ρ is given by relationship [22, 23]:

$$\rho = \pi h \sqrt{\frac{R_1 R_2}{\ln\left(\frac{2}{1-k}\right) \ln\left(\frac{2}{1+k}\right)}} \tag{9}$$

wherein for $R_1 \geq R_2$

$$\frac{R_1}{R_2} = \frac{\ln\left(\frac{1-k}{2}\right)}{\ln\left(\frac{1+k}{2}\right)} \tag{10}$$

while the resistivity for the rectangular sample is given by relationship [22, 24]:

$$\rho = \frac{\pi h}{2} \sqrt{\frac{R_1 R_2}{\ln\left(\frac{1+k}{1-k}\right) \ln\left(\frac{1+k}{2\sqrt{k}}\right)}} \tag{11}$$

wherein for $R_1 \geq R_2$

$$\frac{R_1}{R_2} = \frac{\ln\left(\frac{1+k}{1-k}\right)}{\ln\left(\frac{1+k}{2\sqrt{k}}\right)} \tag{12}$$

where k —the modulus of the complete elliptic integral of the first kind and

$$k = f(R_1, R_2) \quad \forall 0 < k < 1 \tag{13}$$

Surface resistance R_s is given by the following formula:

$$R_s = \rho/h \tag{14}$$

where h —the sample thickness; ρ —the resistivity of anisotropic sample.

4 Results and discussion

Results of resistance measurements for different electrode distances from the sample edge corresponding to variants 1–4 are shown in Figs. 3, 4, 5, 6, 7 and 8.

Distances d_1, d_2, d_3 and d_4 (Figs. 3, 4, 5) between electrode and the nearest circle-shaped fabric edge (see Fig. 2a) were determined and are: $d_1 = 35.9$ mm, $d_2 = 21.7$ mm, $d_3 = 7.6$ mm = d_c , $d_4 = 0.0$ mm.

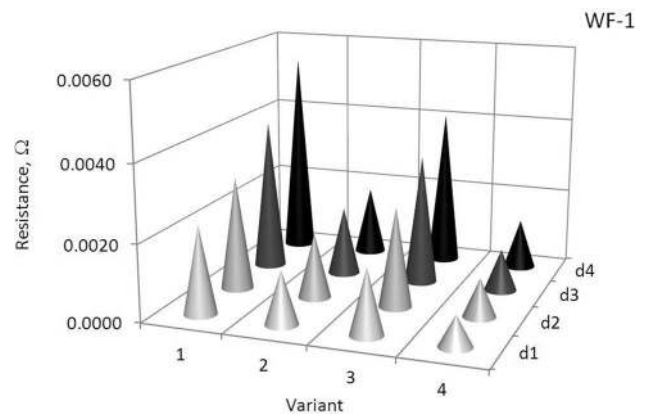


Fig. 3 Results of resistance measurements for fabric WF-1

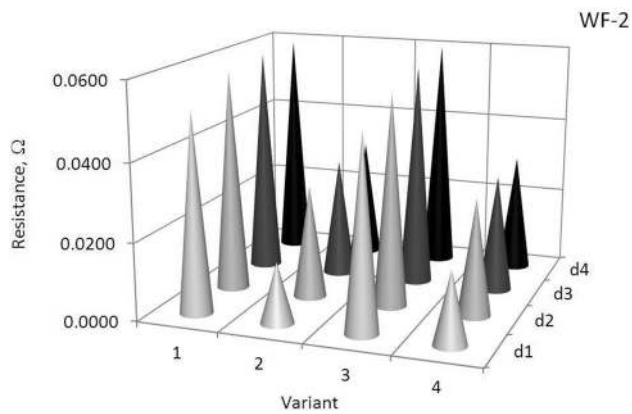


Fig. 4 Results of resistance measurements for fabric WF-2

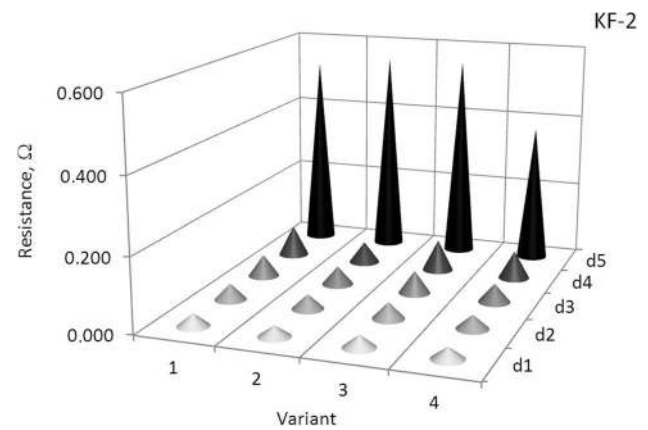


Fig. 7 Results of resistance measurements for fabric KF-2

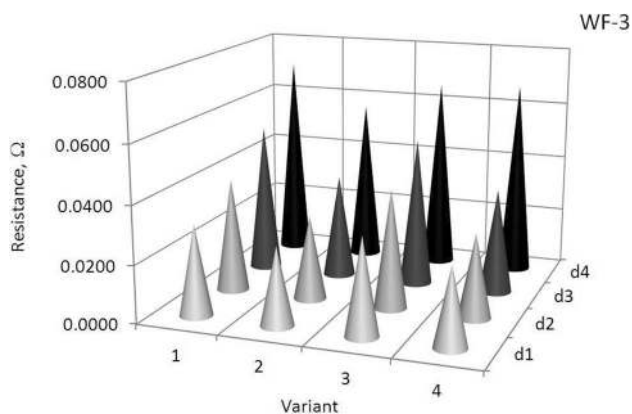


Fig. 5 Results of resistance measurements for fabric WF-3

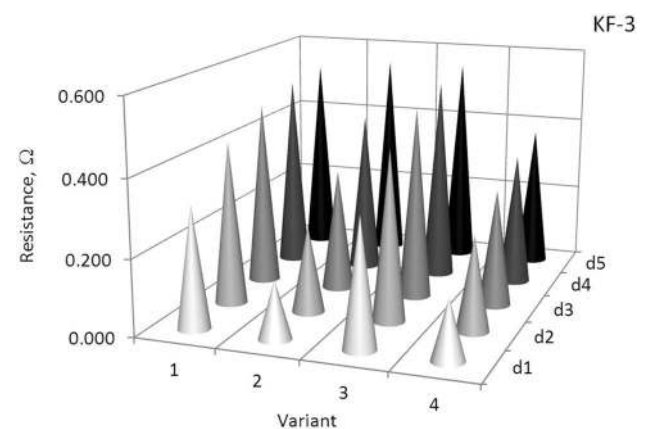


Fig. 8 Results of resistance measurements for fabric KF-3

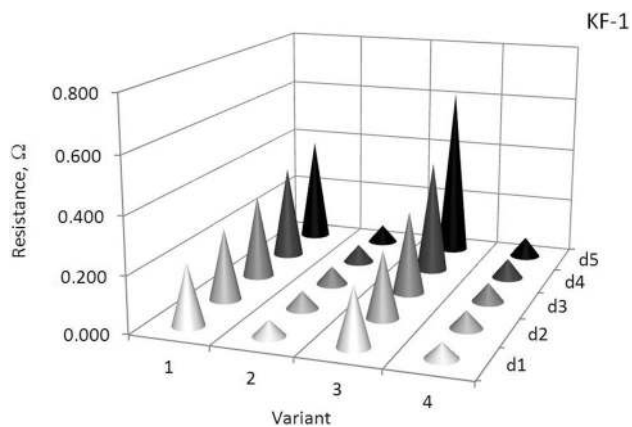


Fig. 6 Results of resistance measurements for fabric KF-1

Distances d_1 , d_2 , d_3 , d_4 and d_5 between electrode and the nearest square-shaped fabric corner (see Fig. 2b) were determined and are: $d_1 = 56.6$ mm, $d_2 = 42.4$ mm, $d_3 = 28.3$ mm = d_r , $d_4 = 14.1$ mm, $d_5 = 0.0$ mm.

In variants 1 and 3, the voltage and current electrodes have been changed. Resistance values are comparable, because in both cases the current flows along warp direction in the case of woven fabric and along course direction in the case of knitted fabric. In variants 2 and 4, the voltage and current electrodes have also been changed. Resistance values are comparable, because in both cases the current flows along weft direction in the case of woven fabric and along wale direction in the case of knitted fabric.

The resistances R_1 and R_2 , the modulus k determined from Eqs. (10) and (12) and the resistivity ρ calculated from Eqs. (9) and (11) for circular sample and square-shaped sample respectively, the surface resistance R_s , calculated from Eqs. (14) and the coefficient R/R are presented in Table 11. The R/R is a biaxial anisotropy coefficient and is calculated as a quotient of higher and lower of resistances R_1 and R_2 .

The values of resistivity obtained for woven and knitted fabrics indicated that the textile materials have electrical resistivity similar to metals or semiconductors. It was found that all fabrics show electrical anisotropy with anisotropy

Table 11 Results of textile materials research

Parameter	WF-1	WF-2	WF-3	KF-1	KF-2	KF-3
R_1 (Ω)	0.002	0.031	0.062	0.070	0.095	0.465
R_2 (Ω)	0.005	0.060	0.069	0.499	0.122	0.541
R/R	3.1	1.9	1.1	7.2	1.3	1.2
k	0.375	0.219	0.033	0.382	0.195	0.187
R_s (Ω)	0.015	0.199	0.297	0.980	0.490	2.276
ρ (Ω cm)	1.75×10^{-4}	1.55×10^{-3}	8.01×10^{-3}	3.88×10^{-2}	1.90×10^{-2}	1.42×10^{-1}

coefficient from 1.1 to 7.2. Influence of warp and weft densities for woven fabrics and course and wale densities for knitted fabrics are presented in Fig. 9.

Values of resistances R_1 and R_2 are dependent on principal axes of textile materials. The main axes in woven fabric were defined by warp and weft directions. The main axes in knitted fabric were defined by course and wale directions. The resistance R_1 was determined when current flows between electrodes arranged on the line parallel to the warp or course direction. It was found that the resistance R_1 is lower than the resistance R_2 where current flows parallel to the weft or wale direction. The higher warp density means occurrence of more contact resistances between warp and weft threads and therefore an increase in woven fabrics resistances (samples WF-1 and WF-2). In case of sample WF-3 it is not so obvious. The comparable values of resistivity R_1 and R_2 (the biaxial anisotropy coefficient R/R was equal to 1.1) may result from a fabric weave other than a plain weave observed in WF-1 and WF-2. The higher course density means occurrence of more contact points of the same thread resulting in occurrence of contact resistances and therefore an increase in all knitted fabrics resistances.

In order to more accurately understand the impact of sample surface roughness on resistances R_1 and R_2 , and surface resistance R_s , a line profile was identified to obtain the basic structural characteristics of fabrics. Two lines of profile were received: the horizontal and the vertical ones (Tables 12, 13) based on TIF file format of images converted into grayscale.

Mean file size was 1957 KB (the coefficient of variation was equal to 3%). Mean resolution of all digital images expressed by pixel count was 995684 pixels (the coefficient of variation was equal to 2%). Line profile was routed through the center of the warp/weft and parallel to the warp/weft direction for woven fabric and through the center of the course/wale and parallel to the course/wale direction for knitted fabric. Measurements were repeated three times and mean values were calculated.

Some important parameters allowing evaluation of sample surface roughness were determined based on received characteristics. Surface area S under the line profile $f(l)$ was calculated using following formula:

$$S = \int_{l_o}^{l_m} f(l) dl \quad l_o \leq l \leq l_m \quad (15)$$

where l —the distance; l_o —the initial distance $l_o = 0$ px; l_m —the final distance.

In formula (15) $l_m = 387$ px was assumed. Surface areas S_h and S_v were calculated corresponding to horizontal and vertical lines respectively using (15). Next spectral analysis was carried out using Statistica® to determine the occurrence of periodicity in the characteristics. The largest peak was identified in periodogram and the corresponding surface roughness frequency fh and period Th for the horizontal

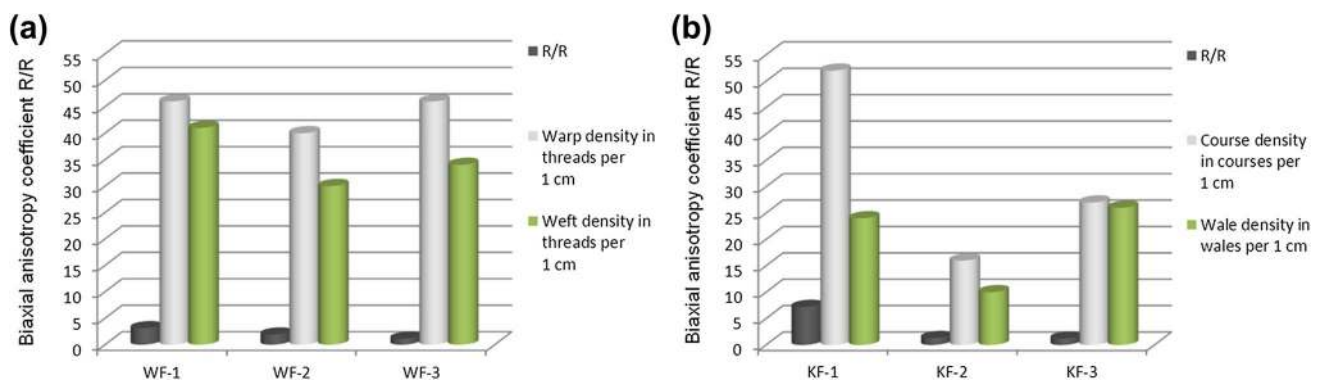
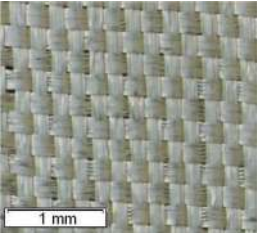
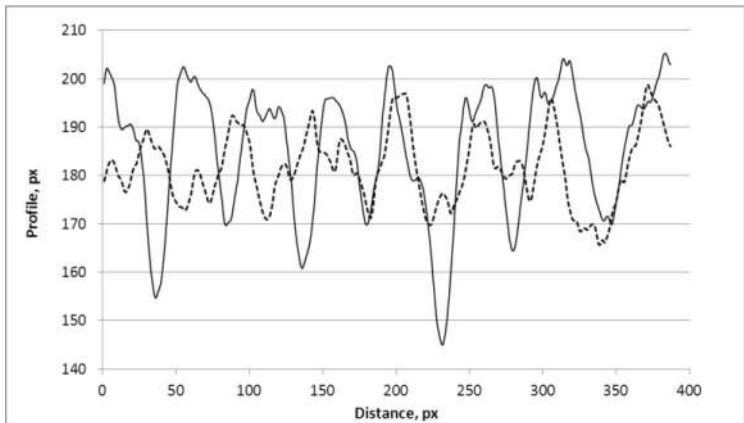
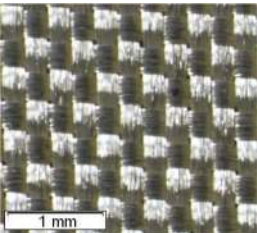
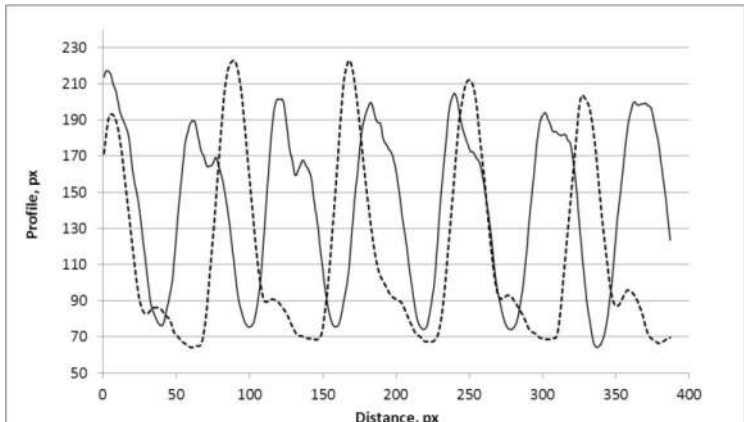
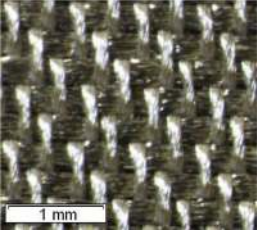
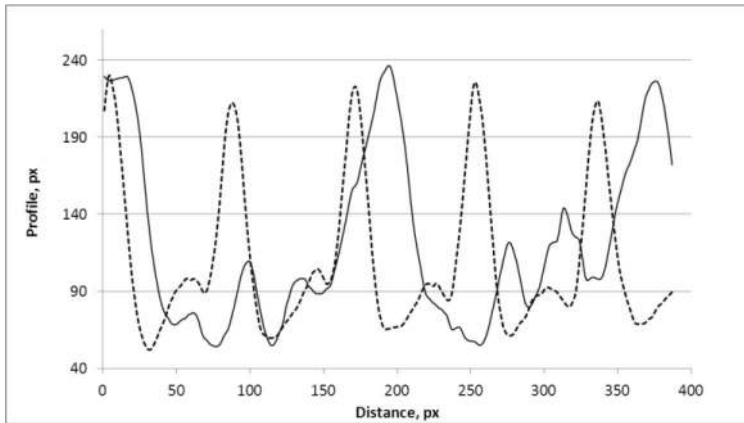
**Fig. 9** a Structure analysis for woven fabrics, b structure analysis for knitted fabrics

Table 12 Surface roughness characteristics for woven fabrics

Microscopic images (1 mm = 120 px) warp direction → weft direction ↓	Lines profiles Horizontal line corresponding to warp direction (the solid line) Vertical line corresponding to weft direction (the dotted line)	Surface roughness parameters
<p>WF-1</p> 		$Sh = 71.521 \text{ px}^2$ $Sv = 70.147 \text{ px}^2$ $fh = 0.021 \text{ 1/px}$ $Th = 48.3 \text{ px}$ $fv = 0.018 \text{ 1/px}$ $Tv = 55.1 \text{ px}$
<p>WF-2</p> 		$Sh = 55.355 \text{ px}^2$ $Sv = 44.620 \text{ px}^2$ $fh = 0.016 \text{ 1/px}$ $Th = 64.3 \text{ px}$ $fv = 0.013 \text{ 1/px}$ $Tv = 77.2 \text{ px}$
<p>WF-3</p> 		$Sh = 46.815 \text{ px}^2$ $Sv = 42.690 \text{ px}^2$ $fh = 0.005 \text{ 1/px}$ $Th = 193.0 \text{ px}$ $fv = 0.013 \text{ 1/px}$ $Tv = 77.2 \text{ px}$

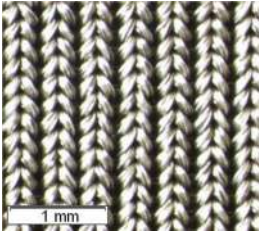
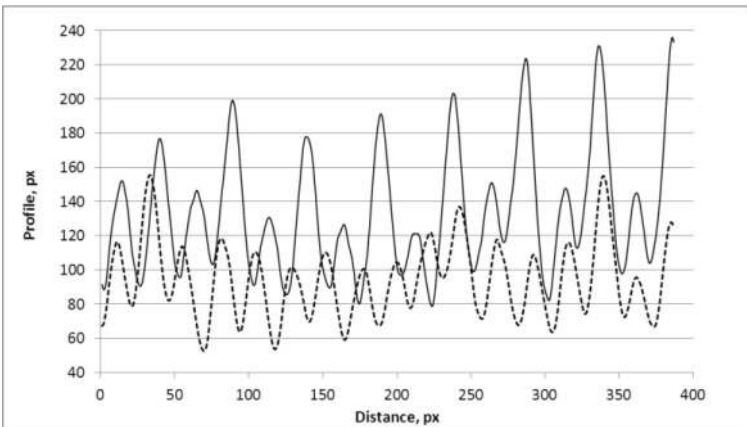
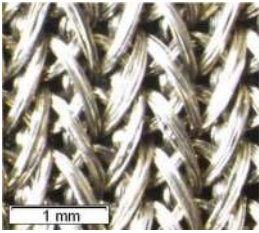
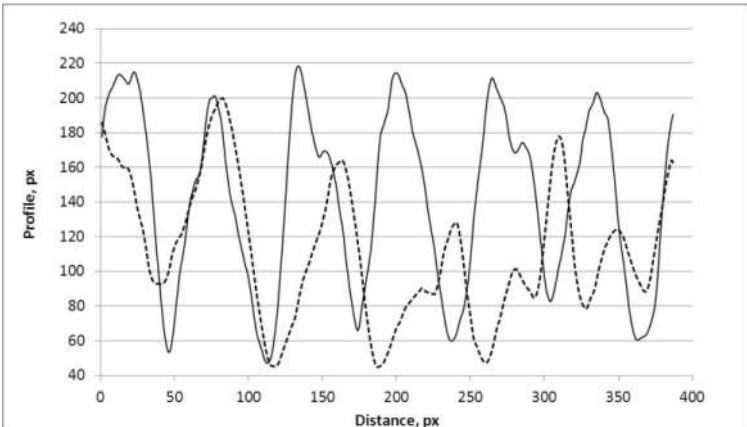
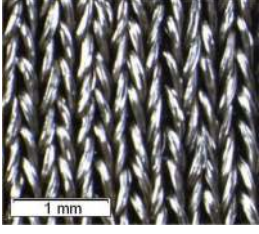
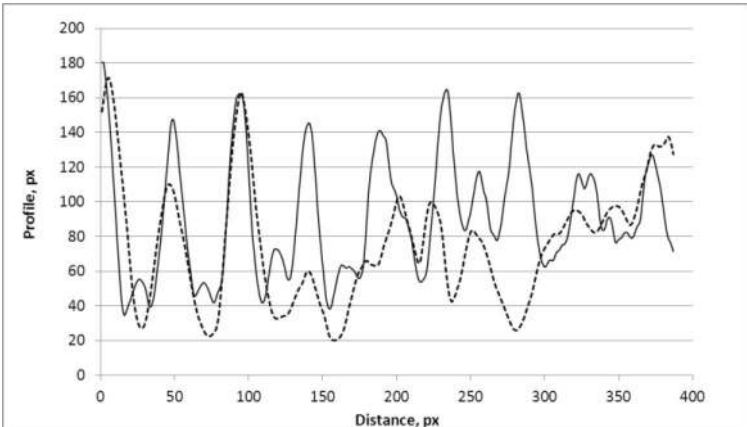
line and fv and period Tv for the vertical line. All calculated parameters are given in Tables 12 and 13.

Pearson's correlation coefficient was used in statistics to measure how strong a relationship is between two parameters characterizing features of textile materials. Pairs of chosen parameters and the corresponding significant values

of Pearson's correlation coefficient (0.05 significance level was assumed) are given in Table 14.

It was found strong downhill linear relationship between the surface area Sh or Sv and the surface resistance R_s . The surface resistance decreases when the surface area increases. The bigger surface area under the function $f(l)$ being the

Table 13 Surface roughness characteristics for knitted fabrics

Microscopic images (1 mm = 120 px) course direction → wale direction ↓	Lines profiles Horizontal line corresponding to course direction (the solid line) Vertical line corresponding to wale direction (the dotted line)	Surface roughness parameters
<p>KF-1</p> 		$Sh = 51.408 \text{ px}^2$ $Sv = 36.398 \text{ px}^2$ $fh = 0.041 \text{ 1/px}$ $Th = 24.1 \text{ px}$ $fv = 0.041 \text{ 1/px}$ $Tv = 24.1 \text{ px}$
<p>KF-2</p> 		$Sh = 54.778 \text{ px}^2$ $Sv = 42.875 \text{ px}^2$ $fh = 0.016 \text{ 1/px}$ $Th = 64.3 \text{ px}$ $fv = 0.028 \text{ 1/px}$ $Tv = 35.1 \text{ px}$
<p>KF-3</p> 		$Sh = 35.279 \text{ px}^2$ $Sv = 28.909 \text{ px}^2$ $fh = 0.021 \text{ 1/px}$ $Th = 48.3 \text{ px}$ $fv = 0.008 \text{ 1/px}$ $Tv = 128.7 \text{ px}$

line profile of the sample means smaller oscillation of the function $f(l)$ and consequently smaller surface resistance. Thus, sample with a smooth surface will conduct electrical current better than sample with a rough one. It was noticed that the greater the disproportion between the densities

(expressed by D) the greater the coefficient R/R . Thus, the textile materials are characterized by higher anisotropy of electro-conductive properties.

Strong uphill linear relationship was observed between the coefficient R/R and the surface roughness frequency fh .

Table 14 Impact of surface roughness parameters on sample electro-conductive properties

Parameter 1	Parameter 2	Pearson's correlation coefficient
R_s	Sh	-0.80
R_s	Sv	-0.74
R/R	D	0.78
R/R	fh	0.90
R/R	fv	0.81

Therefore, if frequency fh corresponding to the largest peak of periodogram obtained for the horizontal line increases the coefficient R/R also increases. Strong uphill linear relationship was also observed between the above coefficient and the surface roughness frequency fv corresponding to the largest peak of periodogram obtained for the vertical line. Results of the conducted analysis confirmed the effect of sample surface roughness on its electro-conductive properties.

5 Conclusions

The main research results of this work are as follows:

- The study shows that the biaxial anisotropy coefficient and the electrical resistivity are very useful in characterizing electrical anisotropy of textile materials. The biaxial anisotropy coefficient indicates whether material property depends on its testing direction with respect to the principal axes.
- Resistance was higher when current flows between electrodes arranged on the line parallel to the warp and course direction in the case of woven or knitted fabrics respectively.
- The value of electrical resistivity makes it possible to qualify textile material in terms of electrical conductivity. The electrical resistivity of the fabrics ranged from $1.75 \times 10^{-4} \Omega \text{ cm}$ to $1.42 \times 10^{-1} \Omega \text{ cm}$. It indicates that they have properties similar to metals.
- Results of analysis of fabrics surface roughness enable the first selection of fabrics from the point of view of its electro-conductive properties. It is also possible to initially conclude on the contact resistance between two linear components in a form of woven or knitted strips intended to design a matrix of pressure sensor.
- The woven fabrics can be used as paths for conveying electrical signals such as textile transmission lines. Moreover they can be used as medical electrodes or e-textile antennas where low resistivity is desired.

Compliance with ethical standards

Conflict of interest Authors declare that they have no conflict of interest.

Open Access This article is distributed under the terms of the Creative Commons Attribution 4.0 International License (<http://creativecommons.org/licenses/by/4.0/>), which permits unrestricted use, distribution, and reproduction in any medium, provided you give appropriate credit to the original author(s) and the source, provide a link to the Creative Commons license, and indicate if changes were made.

References

- J. Leśnikowski, M. Tokarska, *Text. Res. J.* **84**, 290 (2014)
- I. Gil, R. Fernandez-Garcia, J.A. Tornero, *Text. Res. J.* <https://doi.org/10.1177/0040517518770682> (2018)
- X. Zhang, P. Ma, *Autex Res. J.* **18**, 181 (2018)
- M.D. Husain, R. Kennon, T. Dias, *J. Ind. Text.* **44**, 398 (2014)
- J. Zięba, M. Frydrysiak, M. Tokarska, *Fibres. Text. East. Eur.* **19**, 70 (2011)
- S. Maity, A. Chatterjee, *J. Ind. Text.* **47**, 2228 (2018)
- Z. Stempień, T. Rybicki, E. Rybicki, M. Kozanecki, M.I. Szykowska, *Synth. Met.* **202**, 49 (2015)
- D. Depla, S. Segers, W. Leroy, T. Van Hove, M. Van Parys, *Text. Res. J.* **81**, 1808 (2011)
- R.H. Guo, S.X. Jiang, C.W.M. Yuen, M.C.F. Ng, J.W. Lan, *J. Text. I.* **104**, 1049 (2013)
- C.A. Lawrence (ed.) *High Performance Textiles and Their Applications* (Elsevier Ltd., Cambridge, 2014)
- S. Vasile, F. Deruck, C. Hertleer, A. De Raeve, T. Ellegiers, G. De Mey, *Autex Res. J.* **17**, 170 (2017)
- A. Schwarz, J. Hakuzimana, P. Westbroek, G. De Mey, G. Prinitotakis, T. Nyokong, L. Van Langenhove, *Text. Res. J.* **82**, 1587 (2012)
- S.K. Bahadir, S. Jevšnik, *Text. Res. J.* **87**, 232 (2016)
- M. Tokarska, *J. Electron. Mater.* **46**, 1497 (2017)
- M. Tokarska, *J. Mater. Sci.-Mater. Electron.* **27**, 7335 (2016)
- J. Cheng, M. Sundholm, B. Zhou, M. Hirsch, P. Lukowicz, *Pervasive Mob. Comput.* **30**, 97 (2016)
- I. Kazani, G. De Mey, C. Hertleer, J. Banaszczyk, A. Schwarz, G. Guxho, L. Van Langenhove, *Text. Res. J.* **81**, 2117 (2011)
- I. Kazani, G. De Mey, C. Hertleer, J. Banaszczyk, A. Schwarz, G. Guxho, L. Van Langenhove, *Text. Res. J.* **83**, 1587 (2013)
- N.B. Christensen, *Geophys. Prospect.* **48**, 1 (2000)
- N. Martin, J. Sauget, T. Nyberg, *Mater. Lett.* **105**, 20 (2013)
- L.J. Van der Pauw, *Philips Res. Rep.* **13**, 1 (1958)
- J.D. Wasscher, *Electrical Transport Phenomena in MnTe, an Antiferromagnetic Semiconductor* (Technische Hogeschool Eindhoven, Eindhoven, 1969)
- D.S. Kyriakos, N.A. Economou, R.S. Allgaier, *Rev. Phys. Appl.* **15**, 733 (1980)
- D.K. de Vries, A.D. Wieck, *Am. J. Phys.* **63**, 1074 (1995)
- JCGM, *Evaluation of Measurement Data—Guide to the Expression of Uncertainty in Measurement* (JCGM, Geneva, 2008)
- ISO 139:2005, *Textiles—Standard atmospheres for conditioning and testing*
- M. Tokarska, M. Orpel, *Text. Res. J.* <https://doi.org/10.1177/0040517518763978> (2018)